01 Oct 2002

Anaphase Onset does not Require the Microtubule-Dependent Depletion of Kinetochore and Centromere-Binding Proteins

Julie C. Canman

Nitin Sharma

Aaron F. Straight

Katie Shannon
Missouri University of Science and Technology, shannonk@mst.edu

et. al. For a complete list of authors, see https://scholarsmine.mst.edu/biosci_facwork/94

Anaphase onset does not require the microtubule-dependent depletion of kinetochore and centromere-binding proteins

Julie C. Canman[1,‡], Nitin Sharma[1,*], Aaron Straight[2,*], Katie B. Shannon[1], Guowei Fang[3] and E. D. Salmon[1]

[1]University of North Carolina, Department of Biology, 607 Fordham Hall, CB#3280, Chapel Hill, NC 27599, USA
[2]Harvard Medical School, Department of Cell Biology, Seely Mudd 529, 240 Longwood Avenue, Boston, MA 02115, USA
[3]Stanford University, Department of Biological Sciences, Gilbert Building, Room 345, Stanford, CA 94305-5020, USA
*These authors contributed equally to this work
‡Author for correspondence (e-mail: jccanman@email.unc.edu)

Accepted 16 July 2002
Journal of Cell Science 115, 3787-3795 © 2002 The Company of Biologists Ltd
doi:10.1242/jcs.00057

Summary

Spindle checkpoint proteins, such as Mad2 and BubR1, and the motors dynein/dynactin and CENP-E usually leave kinetochores prior to anaphase onset by microtubule-dependent mechanisms. Likewise, 'chromosome passenger proteins' including INCENP are depleted from the centromeres after anaphase onset and then move to the midzone complex, an event that is essential for cytokinesis. Here we test whether the cell cycle changes that occur at anaphase onset require or contribute to the depletion of kinetochore and centromere proteins independent of microtubules. This required the development of a novel non-antibody method to induce precocious anaphase onset in vivo by using a bacterially expressed fragment of the spindle checkpoint protein Mad1 capable of activating the APC/C, called GST-Mad1F10. By injecting PtK1 cells in nocodazole with GST-Mad1F10 and processing the cells for immunofluorescence microscopy after anaphase sister chromatid separation in nocodazole we found that Mad2, BubR1, cytoplasmic dynein, CENP-E and the 3F3/2 phosphoepitope remain on kinetochores. Thus depletion of these proteins (or phosphoepitope) at kinetochores is not required for anaphase onset and anaphase onset does not produce their depletion independent of microtubules. In contrast, both microtubules and anaphase onset are required for depletion of the 'chromosome passenger' protein INCENP from centromeres, as INCENP does not leave the chromosomes prior to anaphase onset in the presence or absence of microtubules, but does leave the centromeres after anaphase onset in the presence of microtubules.

Key words: INCENP, Spindle checkpoint, Mad2, Anaphase, 3F3/2, CENP-E, Dynein, BubR1, Microtubules, Mad1F10, Kinetochore, Centromere

Introduction

Kinetochores perform three major functions in mitosis: (1) they attach to the plus ends of spindle microtubules; (2) they generate forces for chromosome movement; and (3) they prevent anaphase onset until chromosomes are properly attached to the mitotic spindle (Rieder and Salmon, 1998). To perform these functions, unattached kinetochores acquire the microtubule motor proteins cytoplasmic dynein and CENP-E, and the mitotic spindle checkpoint proteins Mps1, Bub1, BubR1, Bub3, Mad1 and Mad2. Motor proteins are thought to be necessary for both attachments of chromosomes to the spindle microtubules and force generation during mitosis. The mitotic spindle checkpoint proteins sense kinetochores that are not attached to microtubules or that lack tension and in response, block progression through anaphase by inhibiting the anaphase promoting complex/cyclosome (APC/C) (Nicklas, 1997). A single unattached kinetochore within a cell is sufficient to trigger this checkpoint (Rieder et al., 1995). Mad2 and BubR1 bind directly to and inhibit the APC/C activator Cdc20, thereby blocking progression through mitosis (Fang, 2002; Tang et al., 2001). Once all the chromosomes attach to the spindle and align at the metaphase plate, checkpoint activity ceases and the APC/C becomes active, inducing sister chromosome separation and segregation by securin protein proteolysis and inducing cytokinesis and exit from mitosis by cyclin B proteolysis (Clute and Pines, 1999; Hoyt, 2001; Millband et al., 2002; Shah and Cleveland, 2000).

Normally, as kinetochores interact with spindle microtubules in prometaphase to form kinetochore microtubules, motor and checkpoint proteins are depleted from kinetochores. Mad2 and cytoplasmic dynein are unique in that they are substantially depleted by anaphase onset, while the other motor and checkpoint proteins are only moderately depleted (Hoffman et al., 2001; Waters et al., 1998). In addition, kinetochore phosphorylation, as detected by 3F3/2 antibody to a phosphoepitope, is turned off as kinetochores become under tension by the net pulling forces of their sister kinetochores towards opposite poles (Gorbsky and Ricketts, 1993; Nicklas et al., 1995). These reduced levels in kinetochore protein concentration and phosphorylation are thought to be important for inactivating the spindle checkpoint and inducing anaphase (Millband et al., 2002; Shah and Cleveland, 2000).

Before anaphase, the centromeric region between sister kinetochores contains high concentrations of a complex of

'chromosome passenger' proteins, including INCENP, aurora B kinase and survivin (Adams et al., 2001). During mitosis, these proteins leave the centromere and re-localize to the cell cortex and the microtubule-rich midzone that forms between separating sister chromatids in anaphase (for a review, see Adams et al., 2001). This change in localization from the centromeres to the midzone complex is essential for cytokinesis (Mackay et al., 1998).

By anaphase onset in mammalian PtK1 tissue cells, a substantial amount of cyclin B1 is degraded indicating a substantial loss of Cdk1-cyclin B1 kinase activity (Clute and Pines, 1999). Thus, it is possible that independently of microtubules, either proteolysis or loss of Cdk1-cyclin B kinase activity could contribute to kinetochore protein localization or tension-dependent kinetochore phosphorylation. To address this issue, we induced anaphase in cells treated with nocodazole to depolymerize all microtubules. We developed a new method to induce anaphase onset in nocodazole-treated cells that does not require microinjection of rabbit antibodies as was used previously to inhibit Mad2 function (Canman et al., 2000; Gorbsky et al., 1998). Here we show that microinjection of a bacterially expressed fragment of Mad1 protein, GST-Mad1F10, induces anaphase with kinetics similar to the anti-Mad2 antibody (Canman et al., 2000). This reagent allowed us to test, by using quantitative immunofluorescence microscopy (Hoffman et al., 2001; King et al., 2000), whether anaphase onset or APC/C activation requires or contributes to the depletion of kinetochore and centromere-binding proteins independently of microtubules.

Materials and Methods

GST-Mad1-F10 protein expression and purification

BL21 *E. coli* cells (a generous gift from Jean-Claude Labbé and Bob Goldstein, UNC-Chapel Hill, NC) were transfected with a plasmid containing the GST sequence (pGEX-4T-1; Amersham Biosciences, Piscataway, NJ) with or without the Mad1F10 sequence (Fig. 1). Cells were then grown at 37°C in LB containing 25 μg/ml kanamycin to an optical density (at 600 nm) of 0.5. Protein expression was induced with 0.2 mM IPTG (Sigma) and cells were grown at 24°C for an additional 3.75-4 hours.

GST alone and GST-Mad1F10 were purified by using GSTrap according to the manufacturer's instructions (Pharmacia Biotech). Purified protein was dialyzed for 24 hours at 4°C with 3 changes into HEK buffer (20 mM Hepes, 100 mM KCl, and 1 mM DTT, pH 7.7 with KOH). After dialysis, GST and GST-Mad1F10 were concentrated to 2 mg/ml by using a YM-30 Microcon centrifugal filter device (Millipore, Bedford, MA), aliquoted into 4 μl aliquots, drop frozen in liquid nitrogen, and stored at –80°C.

In vitro APC/C activation assays

Xenopus egg extracts that had been stably arrested in mitosis by addition of a non-degradable cyclin B protein (cyclin BΔ90) were made as previously described (Desai et al., 1999). To assay for APC/C activity, a radioactive N-terminal fragment of cyclin B (amino acids 1-102) was added. The kinetics of degradation for radioactively labeled cyclin B was then measured in these extracts by SDS-PAGE as described (Fang et al., 1998). When noted (Fig. 2, panel II), Mad2 protein was added at a concentration of 20 μM to arrest the extracts.

Tissue culture, microinjection and time-lapse microscopy

PtK1 cells were cultured as described (Canman et al., 2000) with minor adaptations. F-12 media was used (Sigma) with 10% FBS (Gibco) and half-strength antibiotics (Sigma). Cells were fed every other day and split at 80% confluency. When cells were split, they were first washed with sterile PBS (0.14 M NaCl, 2.5 mM KCl, 10 mM Na_2HPO_4, 1.5 mM KH_2PO_4; pH 7.2) and then washed twice with trypsin EDTA (Sigma). The last trypsin was removed and the cells were allowed to detach at 37°C. Cells were suspended again in F-12 and split into flasks at a 1:3 dilution.

For microinjection experiments, PtK1 cells were grown on coverslips, mounted into modified Rose chambers and microinjected as described previously (Canman et al., 2000). Stage temperature was maintained at ~35°C by using an air curtain incubator (Nevtek, Model ASI 400, Burnsville, VA). Time-lapse images were obtained every 30 seconds by using a MetaView image acquisition system (Universal Imaging, Downingtown, PA) as described (Canman et al., 2000). Cells were microinjected with either 2 mg/ml purified GST or 2 mg/ml GST-Mad1F10 in HEK buffer. Our microinjections typically represent 20% of the cell volume making the intracellular concentration of injected GST-Mad1F10 a maximum of 8 μM (assuming no protein loss or denaturation during handling).

Immunofluorescence

For Mad2, BubR1, INCENP, ACA (anti-centromeric antigens), and cytoplasmic dynein staining, cells were lysed in PHEM (54 mM Pipes, 22.5 mM Hepes, 10 mM EGTA, 8 mM $MgSO_4$, pH 7.0 with KOH) supplemented with 0.5% Triton X-100 for 5 minutes at 37°C. Cells were fixed in 1% formaldehyde in PHEM for 20 minutes at 37°C. For 3F3/2 staining, 100 nM microcystin (Sigma) was added to the lysis buffer and cells were fixed as described above. Following five 3 minute rinses in PHEM, cells were blocked in 6% heat-inactivated donkey serum in PHEM at 25°C for 1 hour. Primary antibody dilutions were performed in 6% boiled donkey serum in PHEM for 45 minutes at 25°C as follows: 1:50 anti-Mad2; 1:500 BubR1 and 1:750 CENP-E (both generous gifts of Tim Yen, Fox Chase Cancer Center, Philadelphia, PA); 1:200 cytoplasmic dynein 70.1 intermediate chain (Sigma); 1:5000 3F3/2 (a generous gift of Gary Gorbsky, The University of Oklahoma Health Sciences Center, Oklahoma City, OK); 1:1000 ACA serum (a generous gift of Kevin Sullivan, The Scripps Research Institute, La Jolla, CA); and 1:1250 anti-INCENP (from A.S.). Following five 3 minute rinses in PHEM-T (PBS supplemented with 0.1% Triton X-100), cells were incubated with appropriate secondary antibodies diluted into 6% heat inactivated donkey serum in PHEM at 25°C for 40 minutes. Secondary minimally crossed donkey antibodies conjugated to either Rhodamine Red X or Cy2 (Jackson ImmunoResearch Laboratories, West Grove, PA) were used at 1:100. After two 3 minute rinses in PHEM-T, cells were incubated with DAPI for 5 minutes. Cells were then rinsed three times for 3 minutes in PHEM-T, rinsed three times for 3 minutes in PHEM and mounted as described previously (Canman et al., 2000).

Fluorescence microscopy

Images of fixed cells were obtained on a Nikon TE300 inverted microscope (Nikon, Melville, NY) with an Orca I camera (Hamamatsu Photonics, Bridgewater, NJ) by using a Nikon 100× 1.4 NA Plan Apochromat phase objective and a Sutter filter wheel for selecting and shuttering of 360, 488 or 568 nm wavelengths as described (Howell et al., 2000). All images were acquired at 0.2 μm steps by using MetaMorph software (Universal Imaging) controlling the Nikon TE300 focus motor. Images were collected by using identical imaging settings. For each group, control images were taken from the same coverslips as the injected cells to control for handling differences. Image processing and figures were made by using PhotoShop 5.5 (Adobe, San Jose, CA).

Fluorescence intensity measurements

Quantification of fluorescence intensities was preformed as described

in detail (Hoffman et al., 2001; King et al., 2000) with the following modifications. Computer generated 21×21 and 30×30 pixel squares (for kinetochore proteins in order to include the entire kinetochore) and 32×32 and 46×46 pixel squares (for INCENP to include the entire centromeric region) were used to measure kinetochore/centromere and background fluorescence (Hoffman et al., 2001). INCENP coverslips were co-stained for ACA to allow precise identification of centromeres. For all other measurements, DAPI staining was used to identify the centromeric region for intensity analysis by using Metamorph software (Universal Imaging) and Microsoft Excel 2000 (Microsoft, Redmond, WA).

Results

GST-Mad1-F10 can activate the APC/C in vitro

Our approach to find a non-antibody mechanism (Canman et al., 2002) to induce precocious anaphase was to use a fragment of human Mad1 called Mad1F10. Mad1F10 contains amino acids 321-556 of Mad1, which includes the Mad1-Mad1 oligomerization domain and the Mad2-binding domain, but is missing the RLK sequence required for Bub1 and Bub3 interaction (Fig. 1). Mad1F10 also lacks the complete kinetochore-association domain found in full length Mad1 (Chung and Chen, 2002). Thus, Mad1F10 was a likely candidate molecule to induce precocious anaphase. We tested this prediction in vitro by using *Xenopus* egg extracts that had been stably arrested in mitosis by addition of a non-degradable cyclin B protein (cyclin BΔ90) (Desai et al., 1999). Mitotic extracts degrade an exogenously added, radioactive N-terminal fragment of cyclin B (amino acids 1-102) with a half-life of 5-10 minutes (Fig. 2, panel I, a). Addition of Mad1F10 (10-60 μM) does not affect the kinetics of degradation (Fig. 2, panel I, b-e). As previously reported, addition of 20 μM Mad2 tetramer inhibits the APC/C and blocks cyclin B degradation (Fang et al., 1998) (Fig. 2, panel II, a). At low levels of Mad1F10 (10-20 μM), the Mad2-treated extracts remained blocked (Fig. 2, panel II, b,c). In contrast, with higher concentrations (40-60 μM) of Mad1F10, the Mad2-dependent checkpoint was inactivated as seen by degradation of radiolabeled cyclin B (Fig. 2, panel II, d,e). Thus, Mad1F10, at high concentrations, can inhibit checkpoint-dependent cell cycle arrest and activate the APC/C in vitro. Similarly, overexpression of full length Mad1 in *Xenopus* egg extracts inactivates the spindle checkpoint (Chung and Chen, 2002). However, Mad1F10 is a more useful tool than Mad1 for inducing anaphase because functional full-length Mad1 is difficult to express in bacteria (G.F., unpublished).

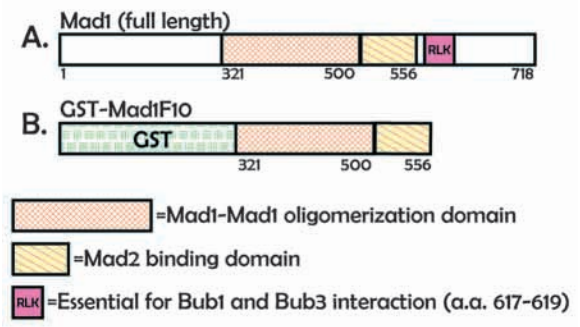

Fig. 1. Mad1 constructs. (A) Full length *Homo sapiens* Mad1 protein showing Mad1-Mad1 oligomerization domain, Mad2-binding domains, and RLK sequence essential for Bub1 and Bub3 interactions. (B) GST-Mad1F10, which lacks the first 320 amino acids of full length Mad1, but contains the Mad1-Mad1 oligomerization domain and the Mad2-binding domain. Notably, GST-Mad1F10 is also missing the last 162 amino acids, which includes the RLK Bub1 and Bub3-interaction sequence.

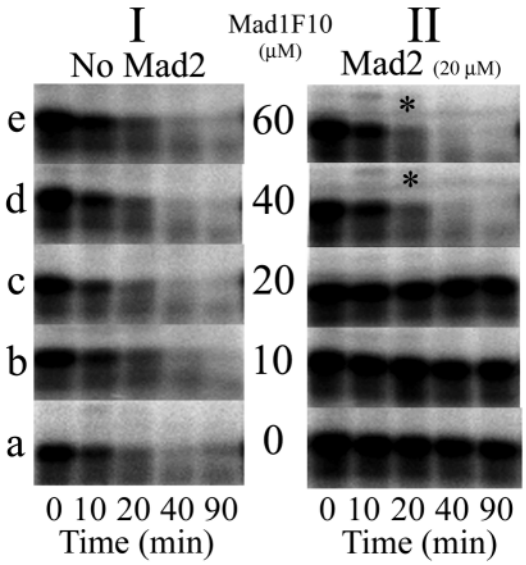

Fig. 2. Mad1F10 can activate the APC/C in vitro. SDS-PAGE of *Xenopus* mitotic extracts that were incubated with buffer alone (panel I) or with 20 μM Mad2 (panel II), in the presence of increasing amounts of Mad1F10 (a-e at 0, 10, 20, 40 and 60 μM). Asterisks indicate APC/C activation by Mad1F10.

GST-Mad1-F10 induces anaphase in early prometaphase and nocodazole-blocked cells

To test the ability of GST-Mad1F10 to inhibit the spindle checkpoint activity in mammalian tissue cells, we microinjected untreated and nocodazole-treated (10 μM) prometaphase PtK1 cells with a needle concentration of 2 mg/ml GST-Mad1F10 in HEK buffer. The untreated prometaphase cells underwent precocious anaphase onset 15±2 minutes after microinjection (n=12, Fig. 3, middle row). Following anaphase onset, all of these injected cells exhibited chromosome segregation and cytokinesis with timing similar to control cells (Fig. 3, top row vs. middle row). The nocodazole-treated cells also underwent precocious anaphase as seen by the separation of sister chromatids (Fig. 3, bottom row). The delay between microinjection and anaphase onset was about twice as long for nocodazole-treated cells, taking 30±5 minutes after microinjection (n=4, Fig. 3). These times to anaphase onset in prometaphase and nocodazole-treated cells are similar to those reported for microinjection of an anti-Mad2 antibody (Canman et al., 2000; Howell et al., 2000). Also, consistent with the anti-Mad2 antibody injection findings (Canman et al., 2000), nocodazole-treated microinjected cells induced to enter anaphase in nocodazole with GST-Mad1F10 underwent cortical contractions followed by cell re-spreading, chromosome decondensation and nuclear envelope reformation; features characteristic of the cytokinetic

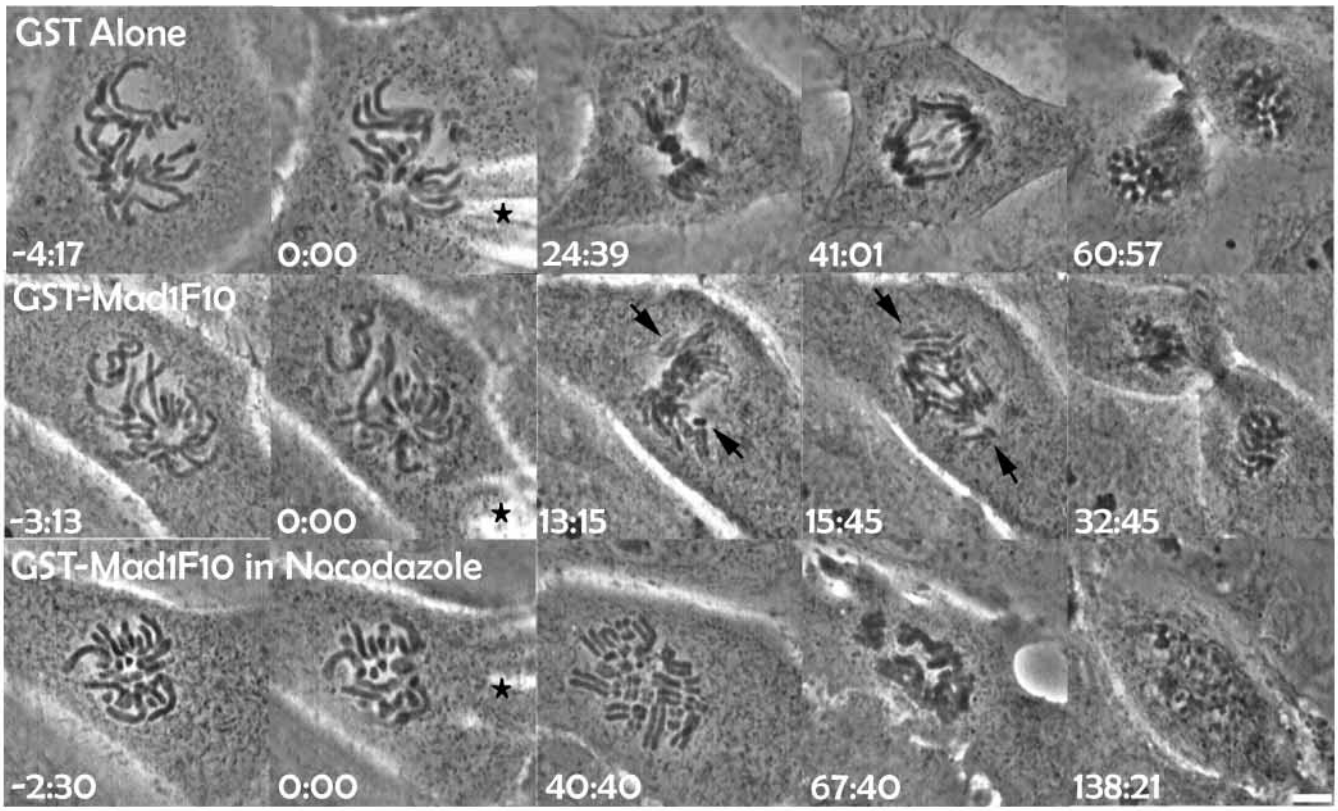

Fig. 3. GST-Mad1F10 can induce premature anaphase onset in prometaphase mammalian tissue cells. Prometaphase PtK1 cells were microinjected with either GST alone (top row) or GST-Mad1F10 (middle row). Microinjection occurred at the 0:00 time point for all rows. The injection of GST-Mad1F10 triggered premature anaphase onset prior to alignment of all chromosomes at the metaphase plate (middle row). Arrows mark unaligned chromosomes. GST-Mad1F10 also induced anaphase onset in cells pre-treated with 10 μM nocodazole to depolymerize all microtubules (bottom row). Asterisks indicates the injection needle. Bar, 5 μM.

phase, or C-phase, of the cell cycle (Fig. 3, bottom row) (Canman et al., 2000). Microinjection of 2 mg/ml GST in HEK buffer alone did not trigger precocious anaphase onset in prometaphase cells (n=10, Fig. 3, top row) or in cells treated with 10 μM nocodazole (n=5, data not shown). Thus GST-Mad1F10, like anti-Mad2 antibody, appears to inactivate the checkpoint without interfering with the mechanics of chromosome segregation or cytokinesis.

Kinetochore cytoplasmic dynein, CENP-E, Mad2, 3F3/2, BubR1 and centromere INCENP are not significantly reduced during anaphase in nocodazole

To test how protein disassembly at kinetochores and centromeres by anaphase depends on microtubules, we analyzed kinetochore protein localization under four experimental conditions: (1) untreated prometaphase cells; (2) untreated prometaphase cells induced into anaphase by GST-Mad1F10 microinjection; (3) prometaphase cells treated with 10 μm nocodazole for 30 minutes to induce depolymerization of all microtubules (Canman et al., 2000); and (4) nocodazole-treated prometaphase cells subsequently induced into anaphase by GST-Mad1F10 microinjection. Individual cells induced into anaphase were followed by time-lapse microscopy and fixed for immunofluorescence analysis after sister chromatid separation. For untreated cells, we compared fluorescence intensities of kinetochores/centromeres between unattached or newly attached chromosomes near the spindle poles, which are expected to have few or no kinetochore microtubules (Hoffman et al., 2001; McEwen et al., 1997), to the values measured for kinetochores/centromeres after induction of precocious anaphase. For cells treated with nocodazole, we compared changes in fluorescence intensities for all kinetochores/centromeres in nocodazole-treated cells before and after induction of anaphase by GST-Mad1F10 injection. It was not possible to compare the differences between the measurements acquired for untreated cells with those acquired for nocodazole-treated cells in these experiments as the experiments were done on different days.

As expected (Gorbsky and Ricketts, 1993; Hoffman et al., 2001), antibodies to Mad2, 3F3/2, cytoplasmic dynein and BubR1 brightly stained unattached or newly attached kinetochores on PtK1 chromosomes in prometaphase, but not the attached and tense kinetochores of chromosomes aligned at the spindle equator (Fig. 4A-D, first rows). All kinetochores in nocodazole-treated cells stained brightly for these kinetochore components (Fig. 4A-D, third rows). By the time untreated prometaphase cells were induced into anaphase, fluorescence was greatly reduced at most kinetochores (Fig. 4A-D, second rows; Table 1A). The average values for Mad2, BubR1, 3F3/2 and dynein fluorescence at untreated anaphase kinetochores decreased to –2%, 6%, 0% and 0% (respectively)

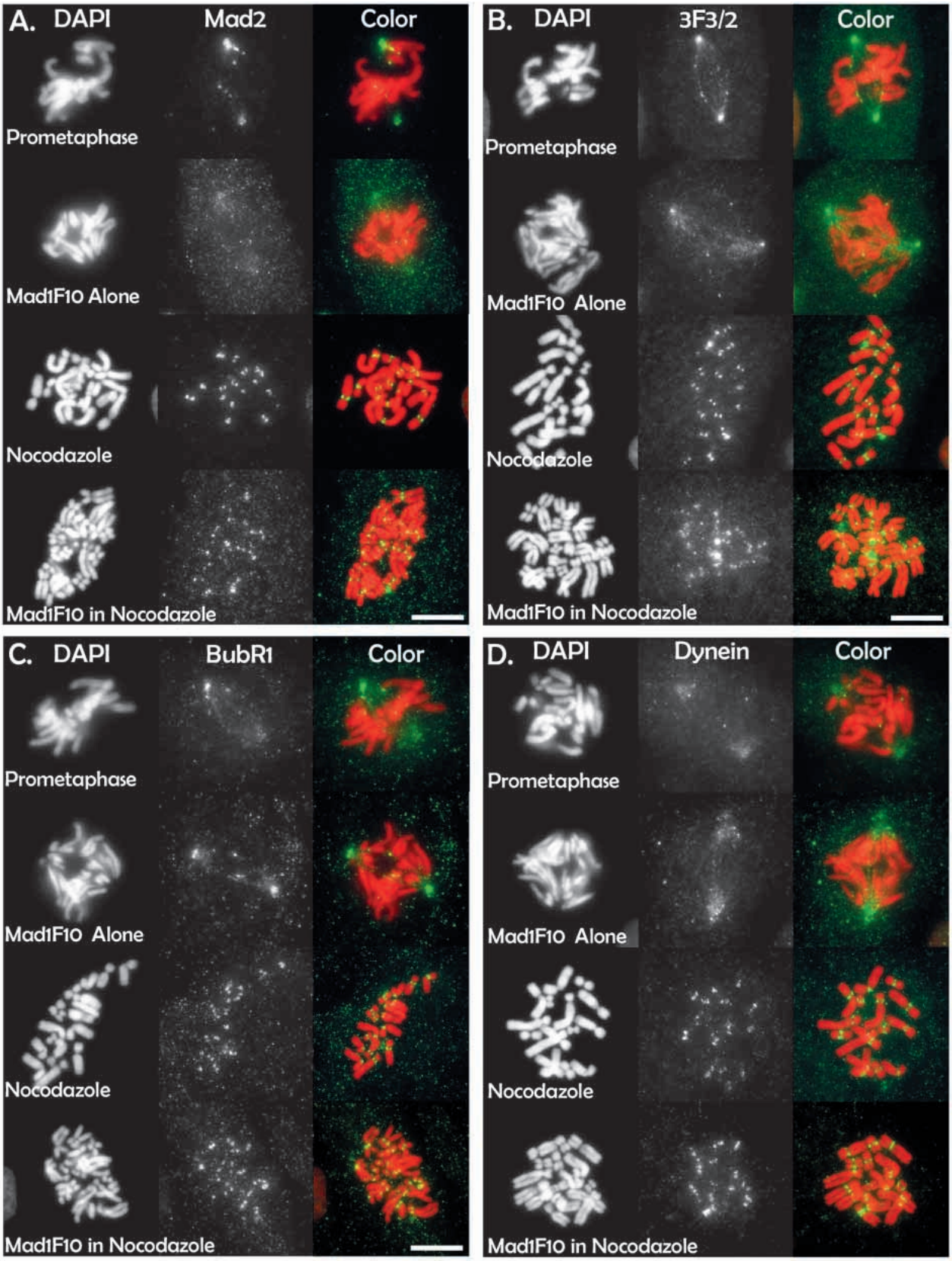

Fig. 4. Microtubules are required for depletion of Mad2, cytoplasmic dynein, BubR1, and the phosphoepitope 3F3/2 at kinetochores in anaphase in PtK1 cells. (A-D) For all images the top row shows a prometaphase cell, the second row shows a cell induced to enter precocious anaphase by Mad1F10 injection, the third row shows a cell treated with 10 μM nocodazole, and the bottom row shows a cell treated with 10 μM nocodazole and induced to enter anaphase by Mad1F10 injection. Bar, 5 μM.

Table 1. Quantification for kinetochore and centromere proteins with and without microtubules

A. PtK1 cells in 10 μM nocodazole

	Mad2	Dynein	3F3/2	BubR1	INCENP	CENP-E
Prometaphase	100±29% *n*=65 kinetochores in 5 cells	100±47% *n*=93 kinetochores in 7 cells	100±34% *n*=101 kinetochores in 5 cells	100±34% *n*=105 kinetochores in 7 cells	100±27%* *n*=86 kinetochores in 6 cells	100±35% *n*=117 kinetochores in 9 cells
Anaphase	39±17% *n*=64 kinetochores in 5 cells	98±42% *n*=96 kinetochores in 6 cells	77±30% *n*=56 kinetochores in 4 cells	84±51% *n*=96 kinetochores in 6 cells	152±64% *n*=117 kinetochores in 8 cells	124±32% *n*=70 kinetochores in 4 cells

B. Control PtK1 cells

	Mad2	Dynein	3F3/2	BubR1	INCENP	CENP-E
Prometaphase	100±44% *n*=13 kinetochores in 5 cells	100±51% *n*=9 kinetochores in 5 cells	100±57% *n*=23 kinetochores in 5 cells	100±62% *n*=14 kinetochores in 4 cells	100±49%* *n*=44 kinetochores in 6 cells	100±51% *n*=78 kinetochores in 8 cells
Anaphase	–2±4% *n*=78 kinetochores in 5 cells	0±22% *n*=101 kinetochores in 6 cells	0±11% *n*=76 kinetochores in 5 cells	6±15% *n*=87 kinetochores in 6 cells	10±19% *n*=89 kinetochores in 7 cells	46±17% *n*=26 kinetochores in 7 cells

*The raw number was reduced by 50% to account for the separation of sister chromatids during anaphase.

Most prometaphase measurements are for unattached or newly attached kinetochores. Kinetochore fluorescence measurements have been corrected for background fluorescence as described in Materials and Methods.

of their average values in prometaphase (Fig. 6; Table 1). In contrast, when a nocodazole-treated cell was induced to enter anaphase, Mad2, 3F3/2, dynein and BubR1 were not substantially reduced (Fig. 4A-D, bottom rows; Table 1B). In the nocodazole-treated cells, average anaphase values for Mad2, BubR1, 3F3/2, and dynein fluorescence at kinetochores after anaphase induction were 39%, 84%, 77%, and 98%, respectively, of their average values in prometaphase (Fig. 6; Table 1). We also quantified changes in kinetochore immunofluorescence for the microtubule motor, CENP-E. Kinetochore-bound CENP-E is reduced by ~50% upon microtubule attachment in prometaphase (Hoffman et al., 2001), but remains at kinetochores in anaphase (Cooke et al., 1997; Yen et al., 1991). CENP-E did not deplete from kinetochores in anaphase in the absence of microtubules (Fig. 6; Table 1). This comparison indicates that microtubules are required in anaphase for the production or maintenance of reduced levels of Mad2, BubR1, dynein and CENP-E, and for the loss of the phosphoepitope recognized by the 3F3/2 antibody at kinetochores.

We next wanted to look at an inner-centromeric protein that is not depleted from centromeres before anaphase onset. INCENP was a prime candidate (Earnshaw and Cooke, 1991). In PtK1 cells, INCENP localized to the centromeric regions of paired sister chromatids in prometaphase (Fig. 5, top row) for both unaligned chromosomes and chromosomes aligned at the spindle equator, and left the centromeres in anaphase [data not shown (see also Adams et al., 2001)]. Thus neither kinetochore microtubule formation nor the centromere tension at aligned chromosomes (Waters et al., 1998) is sufficient to induce the normal depletion of INCENP from the centromere in anaphase. When untreated prometaphase cells were induced to enter anaphase by GST-Mad1F10 injection, INCENP left the centromeres and localized to non-kinetochore microtubules around the kinetochore fibers and also to the midzone microtubule complex that forms between separating chromosomes as expected (Fig. 5, second row). In nocodazole, INCENP was associated with all centromeres (Fig. 5, third row). INCENP also remained at the centromeres when nocodazole-treated cells were induced to enter anaphase by GST-Mad1F10 injection (Figs 5, 6; Table 1). Interestingly,

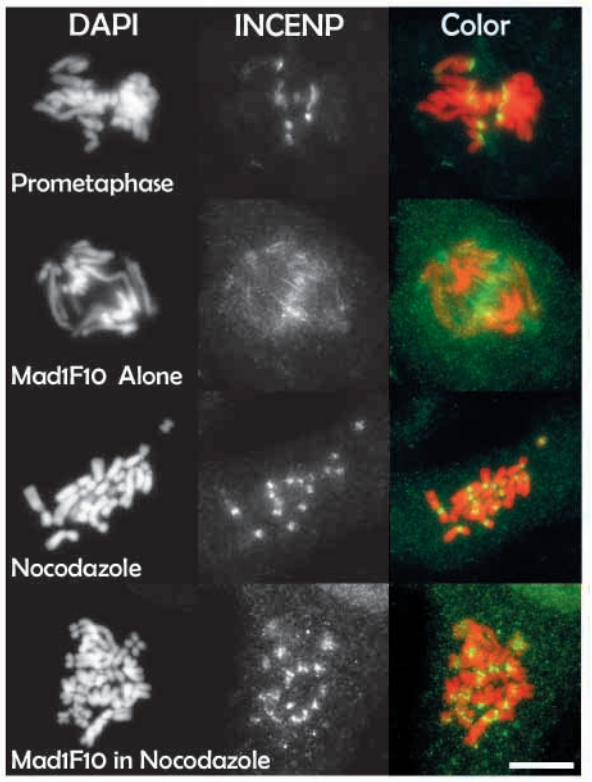

Fig. 5. Microtubules are required for depletion of INCENP at centromeres in anaphase in PtK1 cells. A prometaphase cell fixed and stained for INCENP (top row). A cell induced to enter precocious anaphase by Mad1F10 injection (second row). A cell treated with 10 μM nocodazole (third row). A cell treated with 10 μM nocodazole and induced to enter precocious anaphase by Mad1F10 injection (bottom row). Bar, 5 μM.

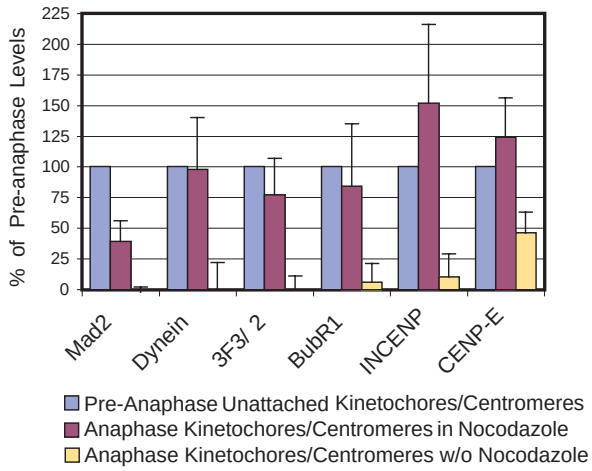

Fig. 6. Kinetochore (Mad2, dynein, 3F3/2, BubR1 and CENP-E) and centromere (INCENP) fluorescence intensity measurements in prometaphase and anaphase with and without microtubules. The figure provides a graphical representation of the data shown in Table 1 after translating the raw measurements to a percentage of unattached prometaphase kinetochore intensities for each experimental condition respectively.

INCENP levels in nocodazole-treated cells increased at centromeres in anaphase, reaching an average 152% of prometaphase level (Fig. 6; Table 1). Thus, INCENP requires both microtubules and the activation of anaphase to become depleted from centromeres.

Discussion

How does GST-Mad1F10 induce precocious anaphase?

GST-Mad1F10 contains amino acids 321-556 of Mad1. This region includes the Mad1-Mad1 oligomerization domain as well as the Mad2-binding domain (G.F., unpublished) (Fig. 1). As Mad1 competes with Cdc20 for the same binding domain on Mad2 (Chen et al., 1999; Luo et al., 2000; Sironi et al., 2001), GST-Mad1F10 at high concentrations likely out-competes Cdc20 for Mad2 binding in a dominant-negative fashion. It is likely this is a cytoplasmic effect as GST-Mad1F10 only partially disrupts Mad2 localization to the kinetochores (Fig. 4A, bottom row; Fig. 6), and it does not stop Mad2 turnover at prometaphase kinetochores in nocodazole (data not shown) as measured by fluorescence recovery after photobleaching (FRAP) analysis (Howell et al., 2000). As GST-Mad1F10 does not contain the kinetochore localization domain present in full length Mad1, this is not surprising (Chung and Chen, 2002). In addition, Mad1F10 lacks the Bub1/Bub3 interaction domain (amino acids 617-619), which is essential for checkpoint maintenance in budding yeast (Brady and Hardwick, 2000). Although, we cannot rule out this and other options, it is likely that GST-Mad1F10 disrupts the spindle checkpoint by sequestering Mad2 from either native Mad1 or Cdc20 or from Mad1-binding sites at the kinetochore (see below).

GST-Mad1F10 is a useful molecular tool for inducing anaphase, as it is not expected to crosslink proteins at kinetochores as occurs with antibody-based mechanisms for precocious anaphase induction (Waters et al., 1998). Therefore, GST-Mad1F10 should be a very useful tool for the analysis of protein function in anaphase and cytokinesis, when functional disruption before anaphase activates the spindle checkpoint (for a review, see Canman et al., 2002).

It is interesting to note that for GST-Mad1 F10 injected cells, as well as for cells injected with anti-Mad2 antibodies (J.C.C. and E.D.S., unpublished) (Canman et al., 2000), the time from microinjection to anaphase onset was significantly longer for nocodazole-treated cells (~22-30 minutes) than for normal prometaphase cells (~9-15 minutes). This difference may be related to the strength of the checkpoint signal generated by the much larger number of unattached (and un-tense) kinetochores in nocodazole-treated cells that have high concentrations of spindle checkpoint proteins (Hoffman et al., 2001).

APC/C activation does not require the depletion of checkpoint proteins from kinetochores

Upon anaphase onset, the sister chromatids separate quickly and are moved to separate poles. The current model to explain the swift shut off of chromosome cohesion upon anaphase onset predicts a feedback loop, with APC/C activity leading to a rapid depletion of checkpoint proteins from their sites of activity at the kinetochores (for a review, see Shah and Cleveland, 2000). Here, however, we clearly showed that anaphase onset does not require the depletion of Mad2, BubR1, dynein or CENP-E. We have also shown that APC/C activity does not require de-phosphorylation of the 3F3/2 phosphoepitope (see also below). Thus, if a feedback mechanism exists between anaphase onset and spindle checkpoint de-activation, it is not required for the APC/C activity needed to activate anaphase. Furthermore, anaphase onset can occur with checkpoint proteins at the kinetochores so it is likely that inactivation of the cytoplasmic pool of spindle checkpoint proteins is sufficient to induce anaphase.

Microtubules are essential for maintaining or promoting protein depletion at kinetochores, even in anaphase

A novel finding in this study is that even after anaphase is induced by APC/C activity, microtubules are required for significant reductions at kinetochores of Mad2, BubR1, the 3F3/2 antigen and dynein. In the nocodazole-treated cells, BubR1 and dynein were only slightly reduced at kinetochores after anaphase onset, while Mad2 was reduced by 61% (Fig. 6, Table 1). The decrease in levels of Mad2 at kinetochores is probably the result of the sequestering of Mad2 by the high concentration of GST-Mad1F10 used to induce anaphase. Nevertheless, this 61% reduction is small relative to the 99+% reduction of Mad2 for attached kinetochores at either metaphase (Hoffman et al., 2001) or anaphase (Fig. 6; Table 1). For Mad2, BubR1 and dynein, kinetochore microtubule formation appears to be the dominant mechanism inducing loss of these proteins from the kinetochore through dynein/dynactin-driven transport of these proteins from kinetochores to the poles along spindle microtubules (Hoffman et al., 2001; Howell et al., 2001; Wojcik et al., 2001). In contrast, un-tense kinetochores with a full complement of kinetochore microtubules are brightly stained by 3F3/2 antibody (Waters et al., 1998) indicating that the kinetochore phosphorylation recognized by this antibody is

mainly turned off by tension (Waters et al., 1998). How microtubule attachment or tension controls steady state amounts of kinetochore motor and checkpoint protein concentrations or kinetochore phosphorylation is still a significant unsolved problem (Nicklas et al., 2001). Nevertheless, our results indicate that the molecular events activated by APC/C activity at anaphase onset, such as proteolysis of securin and cyclin B1, do not make a significant contribution in comparison with that made by kinetochore microtubule formation and tension.

A previous study showed that when cells were induced into anaphase by anti-Mad2 antibody injection and then subsequently released from nocodazole to allow microtubule reassembly 20 minutes after anaphase onset, chromosomes were able to move towards separated poles into two masses (Canman et al., 2000). It was not clear how anaphase kinetochores were able to undergo poleward movement so long after anaphase onset. However, with the data from this paper, we can now deduce that the chromosome poleward movement upon nocodazole washout in anaphase was due to the retention of key kinetochore proteins that interact with spindle microtubules (e.g. cytoplasmic dynein and CENP-E).

Evidence that the phosphoepitope recognized by 3F3/2 is not an inhibitory phosphorylation(s) on APC/C components

3F3/2 staining also persisted at kinetochores after the activation of anaphase in the absence of microtubules. This result indicated that loss of the phosphorylation recognized by the 3F3/2 antibody is dependent on microtubules, and independent of APC/C activation. If the 3F3/2 epitope reflects an inhibitory phosphorylation on component(s) of the APC/C, one would predict that the 3F3/2 antigen would disappear upon anaphase onset, to reflect the activation of the APC/C. Therefore, it is unlikely that the phosphoepitopes recognized by 3F3/2 antibodies are inhibitory sites on kinetochore-bound APC/C components, as has been previously proposed (Daum et al., 2000). It is more likely that 3F3/2 antibodies recognize a phosphoepitope on a tension-sensing component of the spindle checkpoint (Campbell and Gorbsky, 1995), the dephosphorylation of which is not essential for anaphase onset as it remains on kinetochores in anaphase in the absence of microtubules.

Both microtubules and anaphase onset are essential for INCENP depletion at centromeres

Here we show that INCENP depletion from the centromeres in anaphase is a microtubule-dependent process. The release of INCENP from centromeres is important for proper INCENP localization to the midzone-microtubule complex during anaphase and for the completion of cytokinesis (Mackay et al., 1998). Unlike the spindle checkpoint proteins, however, INCENP remains on kinetochore at anaphase onset, even in the presence of microtubules (Figs 5, 6; Table 1). Thus, both microtubules and anaphase onset are required for INCENP to leave the chromosomes.

Wheatley and colleagues have previously reported that INCENP moves to the cell cortex in chicken tissue cells when they are treated with nocodazole after the onset of anaphase (Wheatley et al., 2001). In our hands, however, we do not see INCENP targeting to the cell cortex in cells maintained in nocodazole both before and after anaphase onset (Fig. 5, bottom row, and data not shown). This difference is probably due to the fact that without overcoming the spindle checkpoint, it was not possible to have precise control over the timing of microtubule disruption relative to anaphase onset. That is, INCENP may have already moved to the midzone-microtubule complex prior to microtubule depolymerization in their experiments because they were unable to treat with microtubule disrupting drugs prior to anaphase onset. It is likely that the movement along non-kinetochore fibers towards the midzone is key for proper positioning of INCENP and associated proteins [i.e. survivin and aurora B (for a review, see Adams et al., 2001)].

In our studies, INCENP levels at centromeres increased after anaphase in nocodazole. One interpretation of this finding is that in anaphase, binding of INCENP to centromeres is promoted in order to supply INCENP at centromeres for microtubule transport towards the plus ends of the microtubules in the midzone complex at the equator of the cell. INCENP localization to the microtubule midzone has been proposed to be essential for the completion of cytokinesis (Kaitna et al., 2000; Mackay et al., 1998). MKLP1 (also called CHO1 and ZEN-4) is a kinesin-related protein required for cytokinesis (Kuriyama et al., 2002; Powers et al., 1998; Raich et al., 1998) that moves along microtubules towards plus-ends and localizes to the spindle midzone during cytokinesis (Nislow et al., 1990). This motor has been shown to be required for the proper localization of another passenger protein, aurora B (Severson et al., 2000). As aurora B has also been shown to bind to INCENP (Adams et al., 2000), perhaps MKLP1 is the motor responsible for transporting INCENP from centromeres to the midzone complex in anaphase. It will be interesting to visualize the movement and dynamics of INCENP in vivo and determine whether the change in INCENP localization from the centromeres to the midzone complex is dependent on MKLP1.

We thank Gary Gorbsky for the anti-3F3/2 antibodies, Kevin Sullivan for the anti-ACA antibodies, and Tim Yen for the anti-BubR1 and anti-CENP-E antibodies. We also thank Jean-Claude Labbé and Bob Goldstein for the BL21 cells. J.C.C. thanks Olga Rodrigez, Jonathan Berg and Dick Cheney for their generous help with protein purification; Jean-Claude Labbé, Rebecca Cheeks, Nate Dudley, Bonnie Howell, Chad Pearson, Kerry Bloom and Paul Maddox for helpful protocols, advice and discussion; and Paul Maddox, Lisa A. Cameron, Jennifer G. DeLuca, Jen-Yi Lee and Dale Beach for critical comments on the manuscript. G.F. thanks James Chen for technical assistance. In addition, we thank all members of the Salmon lab and the Fang lab for their assistance and support. E.D.S. is supported by NIH grant GMS24364. G.F. is a Searle Scholar, a Kimmel Scholar in Cancer Research, a recipient of the Beckman Young Investigator Award, and a Burroughs-Wellcome Career Award in Biomedical Sciences. G.F. is also supported by a grant from the National Institutes of Health (GM62852).

References

Adams, R. R., Wheatley, S. P., Gouldsworthy, A. M., Kandels-Lewis, S. E., Carmena, M., Smythe, C., Gerloff, D. L. and Earnshaw, W. C. (2000). INCENP binds the aurora-related kinase AIRK2 and is required to target it to chromosomes, the central spindle and cleavage furrow. *Curr. Biol.* **10**, 1075-1078.

Adams, R. R., Carmena, M. and Earnshaw, W. C. (2001). Chromosomal passengers and the (aurora) ABCs of mitosis. *Trends Cell Biol.* **11**, 49-54.

Brady, D. M. and Hardwick, K. G. (2000). Complex formation between Mad1p, Bub1p and Bub3p is crucial for spindle checkpoint function. *Curr. Biol.* **10**, 675-678.

Campbell, M. S. and Gorbsky, G. J. (1995). Microinjection of mitotic cells with the 3F3/2 anti-phosphoepitope antibody delays the onset of anaphase. *J. Cell Biol.* **129**, 1195-1204.

Canman, J. C., Hoffman, D. B. and Salmon, E. D. (2000). The role of pre- and post-anaphase microtubules in the cytokinesis phase of the cell cycle. *Curr. Biol.* **10**, 611-614.

Canman, J. C., Salmon, E. D. and Fang, G. (2002). Inducing precocious anaphase onset in cultured mammalian cells. *Cell Motil. Cytoskeleton* **52**, 61-65.

Chen, R. H., Brady, D. M., Smith, D., Murray, A. W. and Hardwick, K. G. (1999). The spindle checkpoint of budding yeast depends on a tight complex between the Mad1 and Mad2 proteins. *Mol. Biol. Cell* **10**, 2607-2618.

Chung, E. and Chen, R.-H. (2002). Spindle checkpoint requires Mad1-bound and Mad1-free Mad2. *Mol. Biol. Cell* **13**, 1501-1511.

Clute, P. and Pines, J. (1999). Temporal and spatial control of cyclin B1 destruction in metaphase. *Nat. Cell Biol.* **1**, 82-87.

Cooke, C. A., Schaar, B., Yen, T. J. and Earnshaw, W. C. (1997). Localization of CENP-E in the fibrous corona and outer plate of mammalian kinetochores from prometaphase through anaphase. *Chromosoma* **106**, 446-455.

Daum, J. R., Tugendreich, S., Topper, L. M., Jorgensen, P. M., Hoog, C., Hieter, P. and Gorbsky, G. J. (2000). The 3F3/2 anti-phosphoepitope antibody binds the mitotically phosphorylated anaphase-promoting complex/cyclosome. *Curr. Biol.* **10**, R850-R852.

Desai, A., Murray, A. W., Mitchison, T. J. and Walczak, C. E. (1999). The use of *Xenopus* egg extracts to studey mitotic spindle assembly and function in vitro. *Methods Cell Biol.* **61**, 385-412.

Earnshaw, W. C. and Cooke, C. A. (1991). Analysis of the distribution of the INCENPs throughout mitosis reveals the existence of a pathway of structural changes in the chromosomes during metaphase and early events in cleavage furrow formation. *J. Cell Sci.* **98**, 443-461.

Fang, G. (2002). The checkpoint protin BubR1 acts synergistically with Mad2 to inhibit the Anaphase-Promoting Complex. *Mol. Biol. Cell* **13**, 755-766.

Fang, G., Yu, H. and Kirschner, M. W. (1998). The checkpoint protein MAD2 and the mitotic regulator CDC20 form a ternary complex with the anaphase-promoting complex to control anaphase initiation. *Genes Dev.* **12**, 1871-1883.

Gorbsky, G. J. and Ricketts, W. A. (1993). Differential expression of a phosphoepitope at the kinetochores of moving chromosomes. *J. Cell Biol.* **122**, 1311-1321.

Gorbsky, G. J., Chen, R. H. and Murray, A. W. (1998). Microinjection of antibody to Mad2 protein into mammalian cells in mitosis induces premature anaphase. *J. Cell Biol.* **141**, 1193-1205.

Hoffman, D. B., Pearson, C. G., Yen, T. J., Howell, B. J. and Salmon, E. D. (2001). Microtubule-dependent changes in assembly of microtubule motor proteins and mitotic spindle checkpoint proteins at ptk1 kinetochores. *Mol. Biol. Cell* **12**, 1995-2009.

Howell, B. J., Hoffman, D. B., Fang, G., Murray, A. W. and Salmon, E. D. (2000). Visualization of Mad2 dynamics at kinetochores, along spindle fibers, and at spindle poles in living cells. *J. Cell Biol.* **150**, 1233-1250.

Howell, B. J., McEwen, B. F., Canman, J. C., Hoffman, D. B., Farrar, E. M., Rieder, C. L. and Salmon, E. D. (2001). Cytoplasmic dynein/dynactin drives kinetochore protein transport to the spindle poles and has a role in mitotic spindle checkpoint inactivation. *J. Cell Biol.* **155**, 1159-1172.

Hoyt, M. A. (2001). A new view of the spindle checkpoint. *J. Cell Biol.* **154**, 909-912.

Kaitna, S., Mendoza, M., Jantsch-Plunger, V. and Glotzer, M. (2000). Incenp and an aurora-like kinase form a complex essential for chromosome segregation and efficient completion of cytokinesis. *Curr. Biol.* **10**, 1172-1181.

King, J. M., Hays, T. S. and Nicklas, R. B. (2000). Dynein is a transient kinetochore component whose binding is regulated by microtubule attachment, not tension. *J. Cell Biol.* **151**, 739-748.

Kuriyama, R., Gustus, C., Yerada, Y., Uetake, Y. and Matuliene, J. (2002). CHO1, a mammalian kinesin-like protein, interacts with F-actin and is involved in the terminal phase of cytokinesis. *J. Cell Biol.* **156**, 783-790.

Luo, X., Fang, G., Coldiron, M., Lin, Y., Yu, H., Kirschner, M. W. and Wagner, G. (2000). Structure of the Mad2 spindle assembly checkpoint protein and its interaction with Cdc20. *Nat. Struct. Biol.* **7**, 224-229.

Mackay, A. M., Ainsztein, A. M., Eckley, D. M. and Earnshaw, W. C. (1998). A dominant mutant of inner centromere protein (INCENP), a chromosomal protein, disrupts prometaphase congression and cytokinesis. *J. Cell Biol.* **140**, 991-1002.

McEwen, B. F., Heagle, A. B., Cassels, G. O., Buttle, K. F. and Rieder, C. L. (1997). Kinetochore fiber maturation in PtK1 cells and its implications for the mechanisms of chromosome congression and anaphase onset. *J. Cell Biol.* **137**, 1567-1580.

Millband, D. N., Campbell, L. and Hardwick, K. G. (2002). The awesome power of multiple model systems: interpreting the complex nature of spindle checkpoint signaling. *Trends Cell Biol.* **12**, 205-209.

Nicklas, R. B. (1997). How cells get the right chromosomes. *Science* **275**, 632-637.

Nicklas, R. B., Ward, S. C. and Gorbsky, G. J. (1995). Kinetochore chemistry is sensitive to tension and may link mitotic forces to a cell cycle checkpoint. *J. Cell Biol.* **130**, 929-939.

Nicklas, R. B., Waters, J. C., Salmon, E. D. and Ward, S. C. (2001). Checkpoint signals in grasshopper meiosis are sensitive to microtubule attachment, but tension is still essential. *J. Cell Sci.* **114**, 4173-4183.

Nislow, C., Sellitto, C., Kuriyama, R. and McIntosh, J. R. (1990). A monoclonal antibody to a mitotic microtubule-associated protein blocks mitotic progression. *J. Cell Biol.* **111**, 511-522.

Powers, J., Bossinger, O., Rose, D., Strome, S. and Saxton, W. (1998). A nematode kinesin required for cleavage furrow advancement. *Curr. Biol.* **8**, 1133-1136.

Raich, W. B., Moran, A. N., Rothman, J. H. and Hardin, J. (1998). Cytokinesis and midzone microtubule organization in Caenorhabditis elegans require the kinesin-like protein ZEN-4. *Mol. Biol. Cell* **9**, 2037-2049.

Rieder, C. L. and Salmon, E. D. (1998). The vertebrate cell kinetochore and its roles during mitosis. *Trends Cell Biol.* **8**, 310-318.

Rieder, C. L., Cole, R. W., Khodjakov, A. and Sluder, G. (1995). The checkpoint delaying anaphase in response to chromosome monoorientation is mediated by an inhibitory signal produced by unattached kinetochores. *J. Cell Biol.* **130**, 941-948.

Severson, A. F., Hamill, D. R., Carter, J. C., Schumacher, J. and Bowerman, B. (2000). The aurora-related kinase AIR-2 recruits ZEN-4/CeMKLP1 to the mitotic spindle at metaphase and is required for cytokinesis. *Curr. Biol.* **10**, 1162-1171.

Shah, J. V. and Cleveland, D. W. (2000). Waiting for anaphase: Mad2 and the spindle assembly checkpoint. *Cell* **103**, 997-1000.

Sironi, L., Melixetian, M., Faretta, M., Prosperini, E., Helin, K. and Musacchio, A. (2001). Mad2 binding to Mad1 and Cdc20, rather than oligomerization, is required for the spindle checkpoint. *EMBO J.* **20**, 6371-6382.

Tang, Z., Bharadwaj, R., Li, B. and Yu, H. (2001). Mad2-independent inhibition of APC-Cdc20 by the mitotic checkpoint protein BubR1. *Dev. Cell* **1**, 227-237.

Waters, J. C., Chen, R. H., Murray, A. W. and Salmon, E. D. (1998). Localization of Mad2 to kinetochores depends on microtubule attachment, not tension. *J. Cell Biol.* **141**, 1181-1191.

Wheatley, S. P., Kandels-Lewis, S. E., Adams, R. R., Ainsztein, A. M. and Earnshaw, W. C. (2001). INCENP binds directly to tubulin and requires dynamic microtubules to target to the cleavage furrow. *Exp. Cell Res.* **262**, 122-127.

Wojcik, E., Basto, R., Serr, M., Scaerou, F., Karess, R. and Hays, T. (2001). Kinetochore dynein: its dynamics and role in the transport of the Rough deal checkpoint protein. *Nat. Cell Biol.* **3**, 1001-1007.

Yen, T. J., Compton, D. A., Wise, D., Zinkowski, R. P., Brinkley, B. R., Earnshaw, W. C. and Cleveland, D. W. (1991). CENP-E, a novel human centromere-associated protein required for progression from metaphase to anaphase. *EMBO J.* **10**, 1245-1254.